Fabrication and Testing of All Solid-State Micro-Scale Lithium Batteries for Microspacecraft Applications

W. C. West, J. F. Whitacre, V. White, B. V. Ratnakumar

Electrochemical Technologies Group/Micro Device Laboratories/Center for Integrated Space Microsystems
Jet Propulsion Laboratory
California Institute of Technology
Pasadena, CA 91109

ABSTRACT

A microfabrication process has been developed to prepare thin film solid state lithium batteries as small as 50 μm x 50 μm. Individual cells operate nominally at 3.9 V with 10 μA-hr/cm^2 for a 0.25 μm thick cathode film. The cells are easily fabricated in series and parallel arrangement to yield batteries with higher voltage and/or capacity. Multiple charge/discharge cycles are possible, though an apparent reaction of the in-situ plated Li film with water or oxygen decreases cycle life several orders of magnitude from expected results. Further optimization of an encapsulating film will likely extend the cell cyclability. These microbattery arrays will be useful for providing on-chip power for low current, high voltage applications for microspacecraft and other miniaturized systems.

Introduction

Recent successes in the effort to miniaturize spacecraft components using MEMS technology, integrated passive components, and low power electronics have driven the need for very low power, low profile, low mass micro-power sources for micro/nanospacecraft applications. The miniaturization and integration of power sources with the devices to be powered will enable the concept of distributed sensing for a host of planetary wide-area sampling and exploration missions. This highly integrated approach would be useful for analogous commercial, aerospace, and military applications as well. By providing point-of-use power, significant reductions in the mass associated with wiring and packaging can be obtained. Similar advantages can be gained by co-locating micro-scale batteries and integrated circuits on the same chip. For example, conventional

bandgap voltage reference circuits can be quite large, and are candidates for replacement with micro-scale batteries. Analog sensors, which require careful isolation from digital noise for optimal performance, may also benefit from an on-chip micro-scale battery power.

Although micro-scale, liquid electrolyte based batteries have been reported by others [1], to our knowledge no all solid-state micro-scale battery has been documented. This may be due, in part, to the significant difficulties associated with the microfabrication and testing of solid state Li microbatteries, including water sensitivity of the cathode, anode, and electrolyte. Given the options of liquid or solid electrolytes, the design of microbatteries for a particular application must account for both the strengths and weaknesses of the two systems, as discussed below.

Highly miniaturized systems such as distributed micro-sensors may experience extreme conditions such as elevated or reduced temperature, shock and vibration. Thus, the batteries providing power must be very robust. In the case of space applications, the requirements are particularly severe; an all solid-state materials system would be very desirable. Liquid electrolyte batteries are clearly more prone to leakage, freezing, and boiling under adverse environmental conditions compared with solid electrolyte batteries. Furthermore, in some space applications, long cruise times require electrolytes of exceptionally low reactivity to prevent self-discharge over the time frame of several years. No liquid electrolyte for Li batteries can match the inherent stability of the solid electrolyte, lithium phosphorous oxynitride (Lipon), used in thin film Li batteries. [2] However, the advantages of a solid electrolyte are coupled with the inherent disadvantage of low ionic conductivity relative to liquid electrolyte, by as much as three orders of

magnitude. Low ionic conductivity in the electrolyte translates into low current density during charge and discharge. Nonetheless, research in the field of solid polymer, amorphous, and crystalline electrolytes is very active, with encouraging reports of Li conducting solid electrolytes, in some cases approaching that of liquid electrolytes [3, 4]. Given the relative advantages and disadvantages of both liquid and solid state electrolytes, this group has focused upon developing an all solid state microbattery for space applications.

Experimental

Materials Selection

The options for suitable materials for a micro-scale solid state Li battery are rather limited, given the numerous difficulties encountered with both the high oxidative potentials encountered at the cathode (in excess of 4 V), and the chemical reactivity of metallic Li at the anode. Fortunately, many of these issues have been addressed and reported in the body of literature related to thin film Li batteries [5]. Typically, thin film batteries are prepared by sputtering or evaporating cathode, electrolyte and anode films through a physical mask to define the battery components. Although these types of batteries are sometimes inaccurately referred to as "microbatteries", they typically have areas on the order of 1 cm^2 and are only "micro" scale in thickness.

The highest performance thin film Li battery materials system has been reported by the Oak Ridge National Laboratories (ORNL) group, with high specific capacity, cycle life on the order of 40,000 charge/discharge cycles with minimal capacity fade, and extremely low self discharge [6-8]. The typical ORNL thin film battery system consists

of a RF magnetron sputtered Co adhesion film, Pt cathode current collector, $LiCoO_2$ cathode, $Li_{3.3}PO_{3.8}N_{0.22}$ solid electrolyte (prepared by RF magnetron sputtering Li_3PO_4 in N_2), and either a thermally evaporated Li anode or a sputtered Ni or Cu blocking anode film that serves as a substrate for in-situ Li plating during charging. Our group has used the ORNL thin film battery design as a template for the microbattery development. Several modifications have been incorporated to facilitate microfabrication, as described below.

Fabrication

All micro-battery components were deposited in a planar, three target RF magnetron sputtering chamber, evacuated to a base pressure of less than 2×10^{-6} Torr with a cryo-pump/turbomolecular pumping system. The $LiCoO_2$ sputter target was prepared by uniaxially pressing $LiCoO_2$ powder (Alfa Aesar) mixed with 5 wt% binder (ethylene-propylene-diene monomer, unknown vendor) and sintering at 800°C for one hour. The Li_3PO_4 target was prepared by uniaxially pressing calcined Li_3PO_4 powder (Aldrich) without binder and sintering at 850°C for one hour. A summary of the deposition conditions for all films is shown in Table 1. The photolithography was carried out using a Solitec 3000 mask aligner. The process flow for microbattery fabrication is shown schematically in Figure 1a-f, with the details of the process flow as follows.

On Si <100> substrates, a 2 μm low-stress silicon nitride film was deposited by chemical vapor deposition to provide electrical isolation between the microbattery cells. The substrates were then patterned with negative photoresist (Shin-Etsu hexamethyldisilanzane adhesion promoter, Futurrex NR5-8000 photoresist, Futurrex

RD6 developer) to define the cathode current collectors. On the patterned photoresist, a 10 nm Ti adhesion film was deposited on the substrate, followed by the deposition of a 200 nm Pt film. The wafers were immersed in acetone or photoresist stripper (Futurrex RR2) to remove the photoresist and lift off the excess Ti/Pt film, thereby defining the cathode current collectors, shown in Figure 1b. In some cases, the lift-off was facilitated by briefly immersing the samples in a sonicated acetone bath.

To define the microbattery cathodes, the substrates were again patterned with negative resist, yielding square openings in the photoresist 50 – 100 μm on a side over the cathode current collectors. A film of $LiCoO_2$ was sputtered over the photoresist, and the wafers were immersed in acetone to remove the photoresist and lift off the excess $LiCoO_2$ (Figure 1c). The $LiCoO_2$ films were moisture sensitive, so the lift off procedure was performed in a dry room to prevent moisture condensation in the acetone from contaminating the films. Photoresist stripper could not be used since it reacted with the $LiCoO_2$ film as well. In some cases, following patterning of the cathode features, the substrates were heated to 300°C for one hour to decrease lattice strain and increase grain size of the nanocrystalline as-sputtered $LiCoO_2$ films. Whereas the ORNL process requires 700°C anneal to yield high capacity cathode performance, the 300°C anneal used here is much more amendable to back-end Si processing, at the cost of lower rate capability of the cathode film [9].

The solid electrolyte film was then deposited over the substrates to a thickness of 500-2000 nm. Without breaking vacuum, a 150 nm Ni blocking anode film was subsequently deposited on the solid electrolyte film to protect it from reaction with ambient moisture during removal from the sputter chamber and further photolithography

steps. The Ni film was patterned with positive photoresist (Shipley SJR 5750 photoresist, Shipley Microposit 453 developer). The Ni film was then ion milled in Ar for 20 minutes at 750V and 150 mA to define the Ni anode current collectors and contact pads, shown in Figure 1d.

To open vias in the solid electrolyte over the cathode contact pads, the wafers were patterned with negative resist so that the only unexposed areas on the samples were over the cathode contact pads. When the photoresist was developed, the uncrosslinked resist dissolved leaving the solid electrolyte exposed to the developer solution, which aggressively attacked the solid electrolyte film. The resist was removed with acetone, yielding the unpassivated full cell microbatteries shown in Figure 1e. Alternatively, after the deposition of the electrolyte film, the wafer can be removed from the sputter chamber and patterned and etched to open vias to the cathode current collector. Deposition and patterning of the Ni film is then performed as usual. Using this method, adjacent cells can be patterned in series for multi-cell batteries.

In some cases, an encapsulation film was incorporated into the cell design, as shown in Figure 1f. Presently the encapsulation film employed is a 1 μm sputtered film of Lipon, though a Parylene deposition and patterning process is currently under development in these laboratories.

Testing

Without any encapsulation, the Lipon electrolyte film degrades in humid air after roughly six hours, due to reaction with water vapor, as observed by our group and reported another group [10]. Thus, the samples were stored and tested in a battery dry

room (relative humidity <1%). To make electrical contact to the anode and cathode current collectors, tungsten needles were attached to two micromanipulators and placed in contact with the current collector pads under a stereoscope. The cells were charged and discharged using either a Hewlett Packard 4145B semiconductor parameter analyzer, or a Perkin-Elmer 273A potentiostat/galvanostat, under control by a computer running Corrware software (Scribner Associates).

Results and Discussion

Approximately 20,000 individual microbattery cells per 4" Si wafer are routinely fabricated in roughly six hours of processing time. After charging, each cell operates at nominally 3.9 V and provides 10 μA-hr/cm^2 capacity for a 0.25 μm cathode film at a current density of 10 μA/cm^2. Cells are easily fabricated in parallel and series batteries, as shown in Figure 2. In principle, the battery voltage is limited only by the breakdown voltage of the substrate dielectric film and thus high voltages can be obtained by trivial modifications to the photomask design.

Typical charge and discharge characteristics are shown in Figure 3 for cells with 100 μm x 100 μm active areas. On the charge step, the $LiCoO_2$ cathode is oxidized to approximately $Li_{0.5}CoO_2$, or 4.25 V versus Li/Li$^+$, and the Li$^+$ ions migrate to the anode where they are reduced to form Li metal on the Ni blocking anode. When the cell is discharged, the Li film is oxidized and is consumed to reduce the $Li_{0.5}CoO_2$ film back to $LiCoO_2$. For applications such as an on-chip voltage reference, it is desirable to have a flat discharge curve so that the reference voltage is a weak function of the cell state of charge. Though more than 85% of the capacity of the cell is discharged between 4.25 V

to 2 V (Figure 3), the profile is not flat. Lower discharge rates improve the profile, flattening the curve. By increasing $LiCoO_2$ crystalline size or increasing the $LiCoO_2$ film (104) out of plane texture [9], a flatter discharge profile may be expected. Macroscopic thin film batteries fabricated by this group, and incorporating a 300°C annealing step, have this desired flat discharge profile, as shown in Figure 4 for a 1.7 μm thick cathode film. Further work is underway in addressing the above issues to yield microfabricated cells with suitable discharge profiles for on-chip voltage reference.

On the first cycle, the charge capacity is usually greater than the discharge capacity by roughly 30%. The magnitude of this difference, the irreversible capacity of the cell, decreases with subsequent cycling, as shown in Figure 5. Presumably, both the large irreversible capacity and capacity fade with cycling are due to reaction of the in-situ plated Li film with residual water vapor or oxygen present in the battery testing dry room. When the cells are coated with an encapsulation film, both the irreversible capacity and capacity fade are sharply reduced, as shown in Figure 6. Neudecker et al. [8] report comparable results for macroscopic thin film batteries of very similar design. The authors found that the inclusion of an encapsulation film resulted in decreased irreversible capacity and capacity fade. Furthermore, the authors found that Parylene/Ti based films were superior to Lipon films in protecting the cells from parasitic side reactions with the ambient. Based on these reports, our group is developing Parlyene based encapsulation films for improved cell performance. Further refinements in the wet processing associated with the photolithography steps will also likely improve cycle life. As noted earlier, the cathode, electrolyte, and in-situ plated Li films are all highly

reactive, particularly to water. By minimizing the exposure of these films to wet processing, improvements in cell performance may be expected.

In addition to the improvements in cell performance obtained by including an encapsulation film in the cells, an improvement in both the capacity and discharge voltage was achieved by annealing the cells following deposition of the $LiCoO_2$ film, as shown in Figure 7. As-sputtered $LiCoO_2$ films are typically nanocrystalline and have poor performance in thin film batteries. Annealing at 300°C has been demonstrated to decrease the $LiCoO_2$ lattice strain and increase grain size, resulting in improved electrochemical properties [9].

Conclusions

In concert with the trend of miniaturization of spacecraft components, a microfabrication process has been developed to prepare thin film solid state Li batteries with areas on the order of $(50 - 100\ \mu m)^2$. These cells discharge at 3.9 V with roughly 1 nA-hr capacity for 100 μm x 100 μm cells, and multiple cells may be fabricated in series for higher voltages, or in parallel for higher currents. Unlike comparable Li thin film macroscopic cells, the cycle life is limited to tens of cycles, presumably due to an apparent reaction of the in-situ plated Li film with water or oxygen which decreases cycle life several orders of magnitude from expected results. Whereas macroscopic cells are prepared using physical masking, the microscopic cells are exposed to wet processing during the photolithography process. These processing steps likely contribute to low cycle life due to the introduction of contaminants into the reactive cathode, electrolyte,

and anode films. Further optimization of an encapsulating film and refinement of the wet processing associated with photolithography will likely extend the cell cyclability.

Acknowledgements

This work was carried out at the Jet Propulsion Laboratory, California Institute of Technology, under contract with the National Aeronautics and Space Administration. The authors acknowledge the financial support of the Center for Integrated Space Microsystems of NASA. The authors would like to thank H. Rockstad preparing the silicon nitride films, and S. Surampudi, E. Brandon, and E. Kolawa for providing guidance throughout the project.

References

[1] R. M. LaFollette, J. N. Harb, and R. Humble, *Proc. of IEEE 16th Annual Battery Conf., Long Beach, CA,* 349 (2001), and references therein.
[2] X. Yu, J. B. Bates, G. E. Jellison, and F. X. Hart, *J. Electrochem. Soc.*, **144**, 524 (1997).
[3] A. Hayashi, M. Tatsumisago, and T. Minami, *J. Electrochem. Soc.*, **146**, 3472 (1999).
[4] K. Takada, K. Iwamoto, and S. Kondo, U.S. Patent # 6,210,836.
[5] See for example: J. B. Bates, N. J. Dudney, B Neudecker, A. Ueda, C. D. Evans, *Solid State Ionics*, **135**, 33 (2000); S. D. Jones and J. R. Akridge, *Solid State Ionics*, **69**, 357 (1994).
[6] B. Wang, J. B. Bates, F. X. Hart, B. C. Sales, R. A. Zuhr, and J. D. Robertson, *J. Electrochem. Soc.*, **143**, 3203 (1996).
[7] X. Yu, J. B. Bates, G. E. Jellison, and F. X. Hart, *J. Electrochem. Soc.*, **144**, 524 (1997).
[8] B. J. Neudecker, N. J. Dudney, and J. B. Bates, *J. Electrochem. Soc.*, **147**, 517 (2000).
[9] J.F. Whitacre, W.C. West, E. Brandon, and B.V. Ratnakumar, *accepted for publication in J. Electrochem. Soc.,* 2001.
[10] P. Birke, W. F. Chu, and W. Weppner, *Solid State Ionics*, **93**, 1 (1997).

Table 1. RF magnetron sputter deposition conditions.

Film	Target	Sputter Target Power Density (W/cm^2)	Sputter gas	Deposition pressure (mTorr)	Nominal thickness (nm)
Ti	Ti	6.6	Ar	10	10
Pt	Pt	6.6	Ar	10	200
$LiCoO_2$	$LiCoO_2$	2.2	25% O_2 75% Ar	10	250
LiPON	Li_3PO_4	2.2	N_2	15	500-2000
Ni	Ni	5.5	Ar	10	150

Figure captions:

Figure 1. Schematic process flow for microfabricated batteries.
Figure 2. Micrograph of a five cell serial battery. The outer square features are pads for electrical contact, and the overlapping smaller squares are the active sections of the battery.
Figure 3. Charge/discharge characteristics of 100 μm x 100 μm cells.
Figure 4. Discharge characteristics of an optimized macroscopic thin film cell.
Figure 5. Irreversible capacity fade as a function of cycle number.
Figure 6. Effect of annealing on discharge profile.
Figure 7. Capacity fade for cells with and without a Lipon encapsulation film.

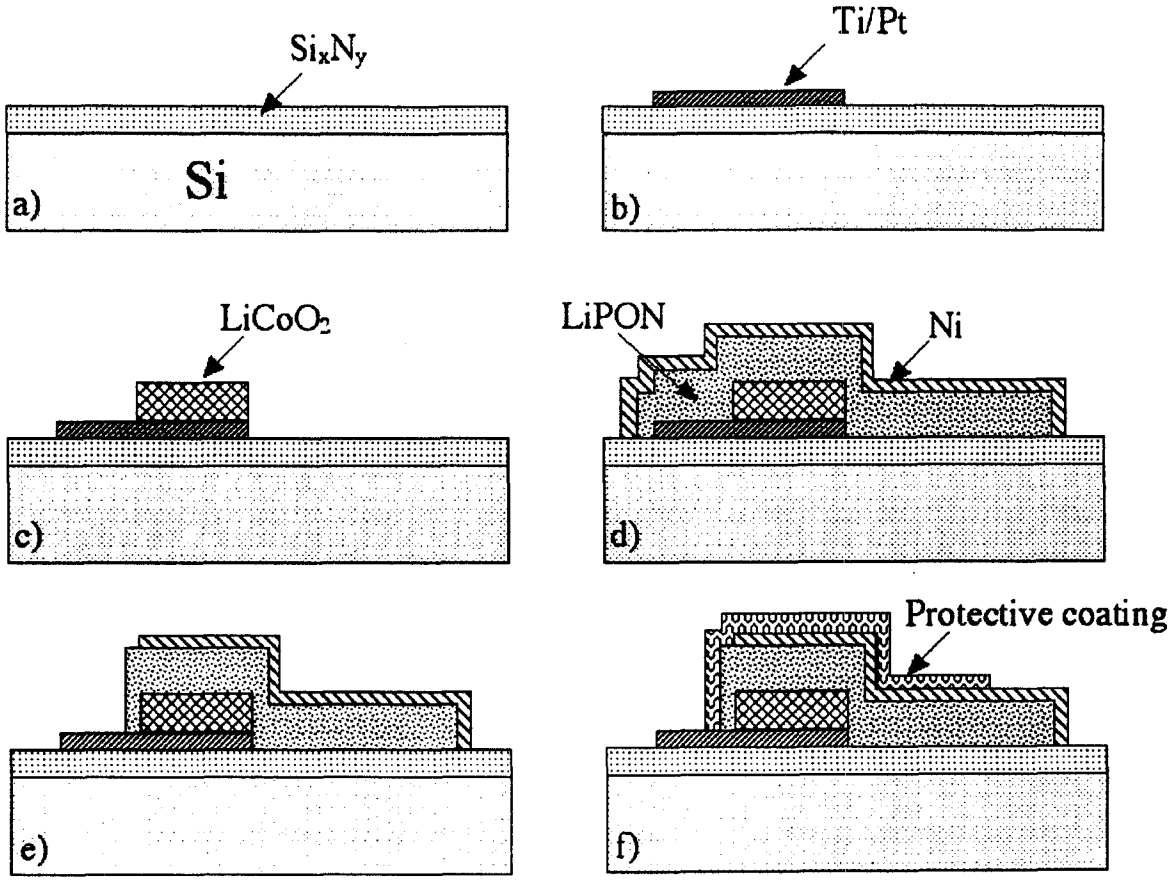

Figure 1.

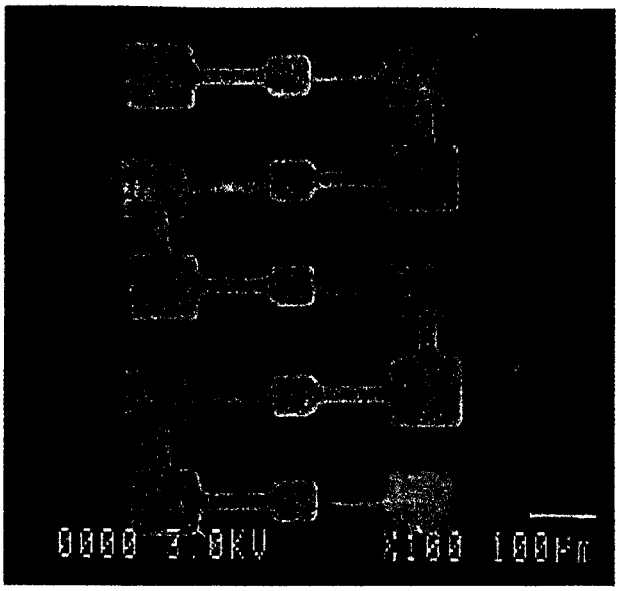

Figure 2.

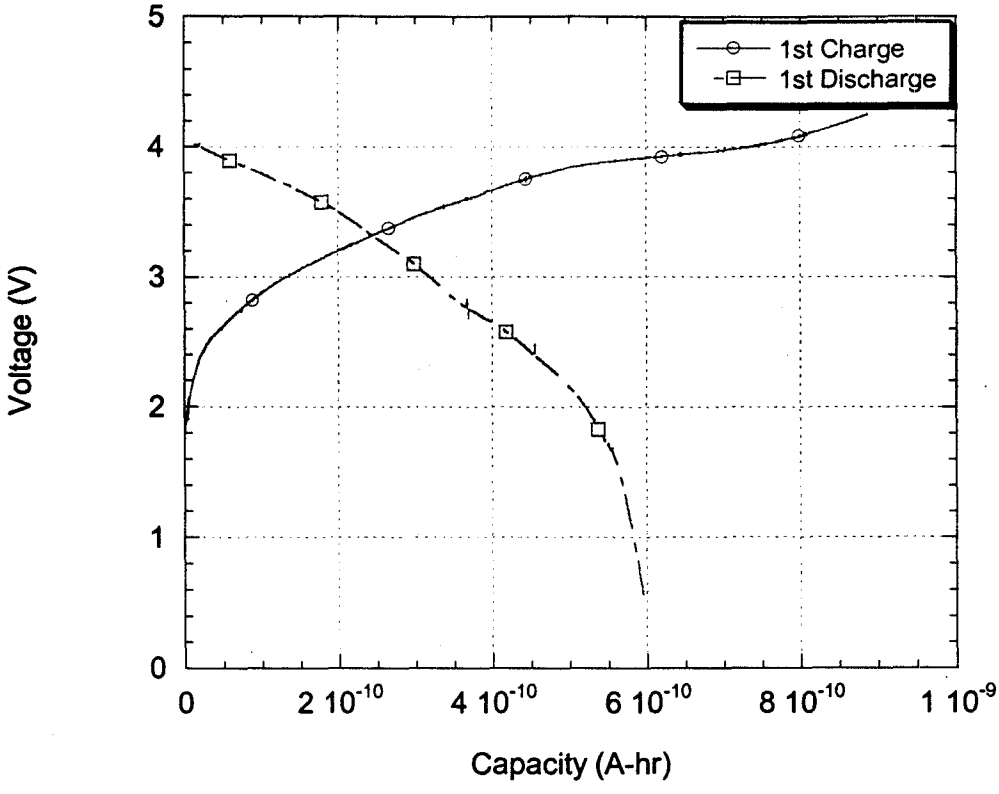
1st Charge
1st Discharge
Voltage (V)
Capacity (A-hr)
0
1
2
3
4
5
0
2 10-10
4 10-10
6 10-10
8 10-10
1 10-9

Figure 3.

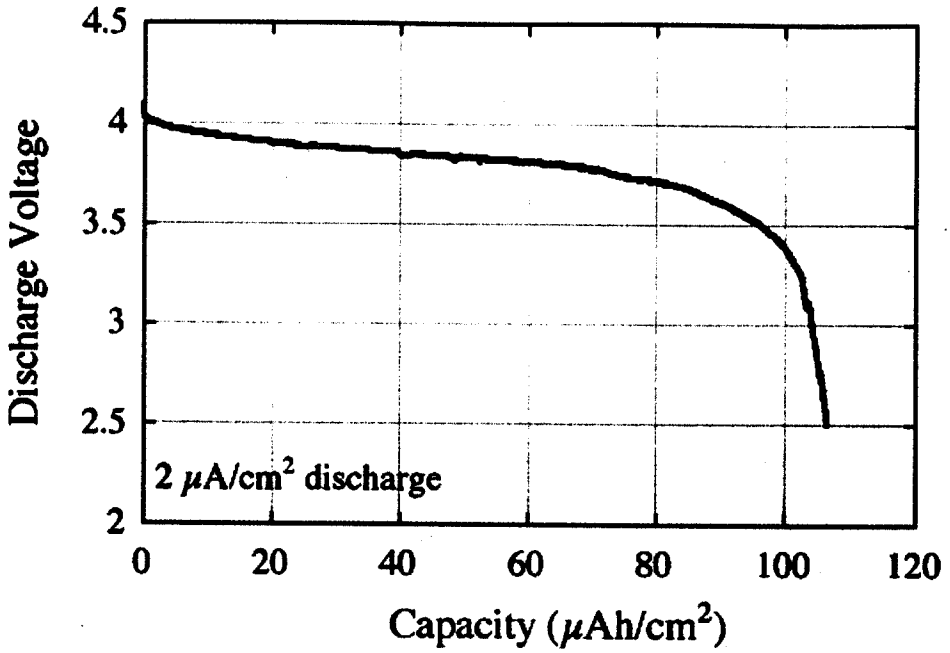
4.5
4
3.5
3
2.5
2
Discharge Voltage
2 μA/cm² discharge
0
20
40
60
80
100
120
Capacity (μAh/cm²)

Figure 4.

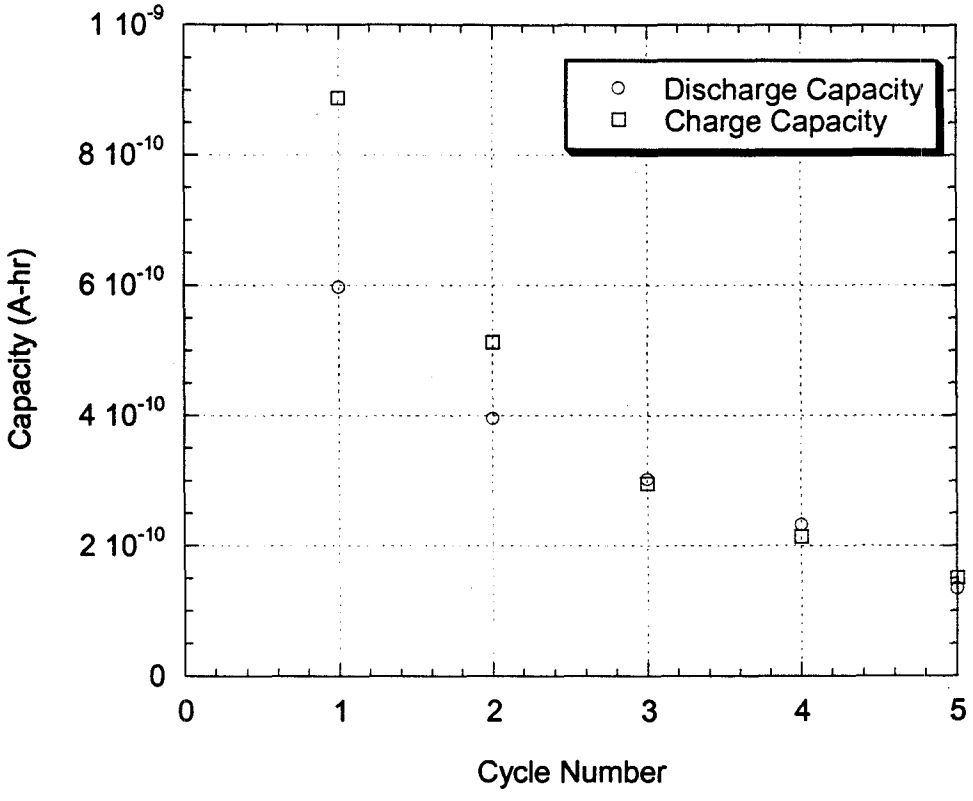
1 10-9
8 10-10
6 10-10
4 10-10
2 10-10
0
Capacity (A-hr)
0
1
2
3
4
5
Cycle Number
Discharge Capacity
Charge Capacity

Figure 5.

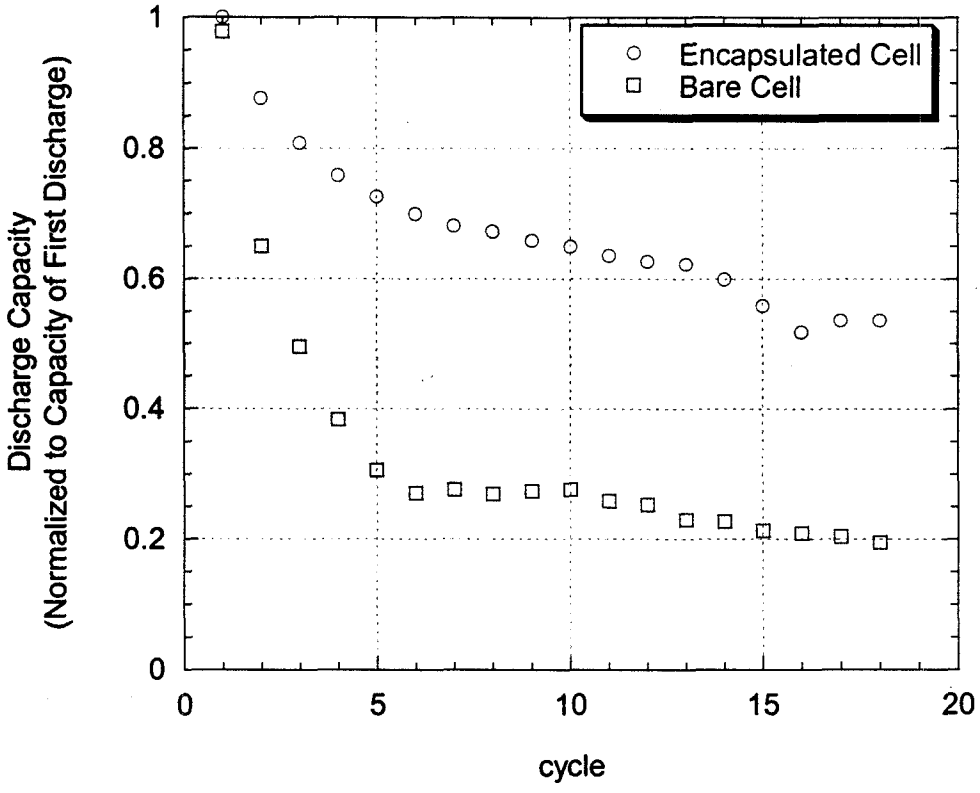
Discharge Capacity
(Normalized to Capacity of First Discharge)
1
0.8
0.6
0.4
0.2
0
0
5
10
15
20
cycle
Encapsulated Cell
Bare Cell

Figure 6.

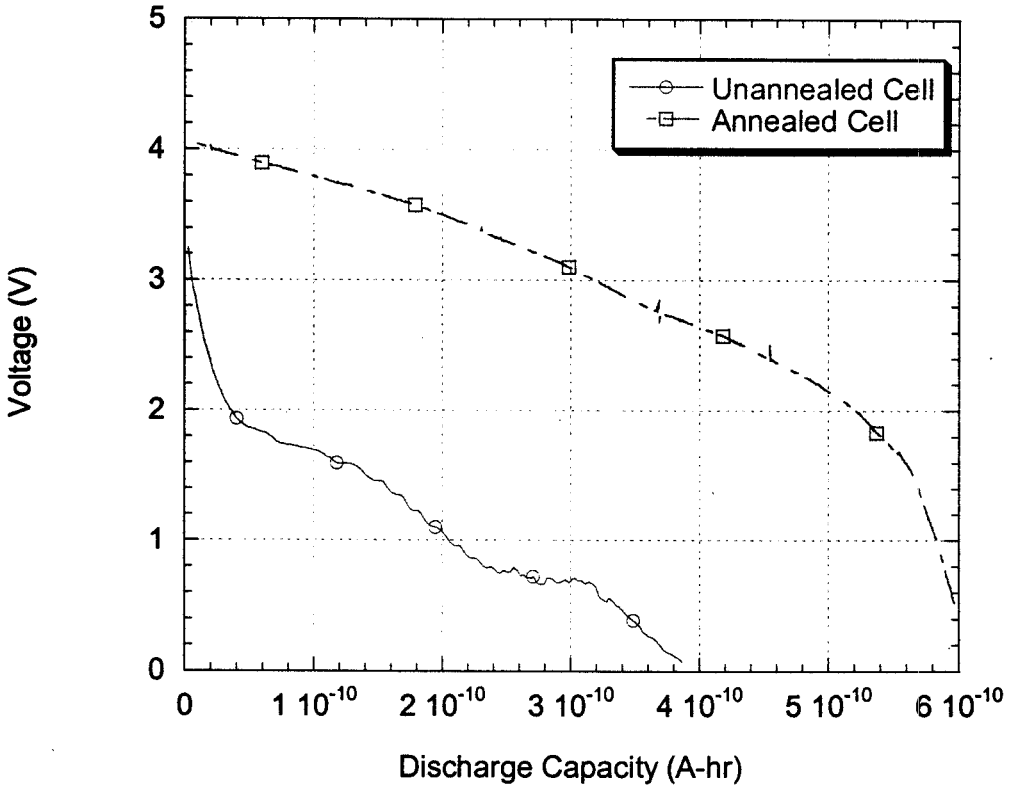
Unannealed Cell
Annealed Cell
Voltage (V)
Discharge Capacity (A-hr)
0
1
2
3
4
5
0
1 10-10
2 10-10
3 10-10
4 10-10
5 10-10
6 10-10

Figure 7.